JOURNAL OF SOLID STATE CHEMISTRY **141,** 255–261 (1998)
ARTICLE NO. SC987976

Reexamination of Protonic Locations in Hydrogen Molybdenum Bronze, H_xMoO_3

Kazuo Eda[1] and Noriyuki Sotani

Department of Chemistry, Faculty of Science, Kobe University, Nada-ku, Kobe 657-8501, Japan

Masakazu Kunitomo

Department of Physics, Faculty of Science, Kobe University, Nada-ku, Kobe 657-8501, Japan

and

Makoto Kaburagi

Department of Communication Studies, Faculty of Cross-Cultural Studies, Kobe University, Nada-ku, Kobe 657-8501, Japan

Received February 23, 1998; in revised form July 14, 1998; accepted July 24, 1998

We reexamined the protonic locations in the phase of hydrogen molybdenum bronze ($H_{0.26}MoO_3$) with the lowest hydrogen content by lineshape analysis using a computer simulation, in which we dealt with systems containing more than three protons. NMR spectra were simulated for various models with a variety of protonic arrangements and linear combinations of the models were tested for whether they could reproduce observed spectra. Spectra for the six-proton cluster models, which were suggested for $H_{0.33}MoO_3$ by Adams *et al.* (*Acta Crystallogr. Sect. B* 49, 958 (1993)), were also simulated. Then, it was suggested that 3- to 5-proton clusters existed in the bronze. © 1998 Academic Press

INTRODUCTION

Hydrogen molybdenum bronze is a hydrogen insertion compound of molybdenum trioxide. As is well known, the bronze exhibits four types of phase with homogeneity of approximate limits (1–5): type I (blue orthorhombic, $0.21 < x < 0.40$), type II (blue monoclinic, $0.85 < x < 1.04$), type III (red monoclinic, $1.55 < x < 1.72$), and type IV (green monoclinic, $x = 2.0$). The location and mobility of hydrogen in the bronze are of general interest for material science and have been investigated extensively by inelastic neutron scattering (INS) (6–10), neutron diffraction (6, 11, 12) and proton nuclear magnetic resonance (NMR) (13–20). We have also studied the NMR spectra of all the phases and tried to interpret them by lineshape analysis using a computer simulation (20). Then, we have clearly shown that the spectra of types II–IV are superpositions of Pake-doublets, a Gaussian, and a Lorentzian, which are attributed to paired protons, isolated and immobile protons, and mobile protons, respectively. For type I, on the other hand, we showed that clustering of protons, such as the three-proton cluster suggested by Ritter *et al.* (17, 18), were important. However, at that time, we could not simulate the spectra of systems containing more than three protons and did not examine the possibility of more than three-proton cluster. We have felt that there is still room for improvement of the fitting between the observed and simulated NMR spectra for this phase. Recently, Adams *et al.* (21) have reported that $H_{0.33}MoO_3$, which belongs to phase I, exhibits a metal–semiconductor transition at 380 K, the origin of which is suggested to be an order–disorder transition of the protons (22), and that the long-range proton ordering, leading to formation of six-proton clusters, is suggested to occur below 380 K from an indirect structural analysis. In the present work, we calculated simulation spectra for a variety of clustering models, including the six-proton clusters, and examined directly the possibility of clustering of more than three protons in type I from the observed proton-NMR spectra.

[1]To whom correspondence should be addressed.

EXPERIMENTAL

Sample Preparation and Characterization

The hydrogen molybdenum bronze was prepared by the method described previously (5). It was confirmed for the sample to be a single phase by powder X-ray diffraction and chemical analysis. The composition of the sample used for NMR measurements was $H_{0.26}MoO_3$.

0022-4596/98 $25.00

NMR Measurements

Proton NMR was detected at liquid nitrogen temperature (77 K) using a pulsed NMR spectrometer operating at 11 MHz. Absorption spectra were obtained by Fourier transformation of the solid echo signals obtained by using the zero-time-resolution method, as described previously (19, 20).

LINESHAPE ANALYSIS

Computer Simulation of NMR Spectra

The Hamiltonian for the interaction of n nuclei consists of the terms of Zeeman and the dipolar interactions, as given by the equation

$$\hat{H} = \hat{H}^{\text{Zeeman}} + \hat{H}^{\text{Dipolar}}. \quad [1]$$

The Zeeman and dipolar terms are, respectively, given as follows:

$$\hat{H}^{\text{Zeeman}} = -\gamma\hbar\mu_0 H_0 \sum_{i=1}^{n} \hat{I}_{iz} \quad [2]$$

$$\hat{H}^{\text{Dipolar}} = \frac{\mu_0\gamma^2\hbar^2}{4\pi} \sum_{i<j} \frac{1}{r_{ij}^3}(A_{ij} + B_{ij} + C_{ij} + D_{ij} + E_{ij} + F_{ij}), \quad [3]$$

where $A_{ij} = \hat{I}_{iz}\hat{I}_{jz}(1 - 3\cos^2\theta_{ij})$, $B_{ij} = -\frac{1}{4}(\hat{I}_{i+}\hat{I}_{j-} + \hat{I}_{i-}\hat{I}_{j+})(1 - 3\cos^2\theta_{ij})$, $C_{ij} = -\frac{3}{2}(\hat{I}_{i+}\hat{I}_{jz} + \hat{I}_{iz}\hat{I}_{j+})\sin\theta_{ij}\cos\theta_{ij}\cdot e^{-i\phi_{ij}}$, $D_{ij} = -\frac{3}{2}(\hat{I}_{i-}\hat{I}_{jz} + \hat{I}_{iz}\hat{I}_{j-})\sin\theta_{ij}\cos\theta_{ij}\cdot e^{i\phi_{ij}}$, $E_{ij} = -\frac{3}{4}\hat{I}_{i+}\hat{I}_{j+}\sin^2\theta_{ij}\cdot e^{-2i\phi_{ij}}$, $F_{ij} = -\frac{3}{4}(\hat{I}_{i-}\hat{I}_{j-}\sin^2\theta_{ij}\cdot e^{2i\phi_{ij}}$, and $(r_{ij}, \theta_{ij}, \phi_{ij})$ denotes the vector joining nuclei i and j, where r_{ij} is the separation between the nuclei and θ_{ij} and ϕ_{ij} are polar angles of the vector against the direction vector of the external field. The terms C_{ij}–F_{ij} have no effect on the spectra (23) and can be ignored in our simulation procedure. Thus, the Hamiltonian could be written as

$$\hat{H} = -\gamma\hbar\mu_0 H_0 \sum_{i=1}^{n} \hat{I}_{iz} + \frac{\mu_0\gamma^2\hbar^2}{4\pi} \sum_{i<j} \frac{1}{r_{ij}^3}(A_{ij} + B_{ij}). \quad [4]$$

The matrix elements of the Hamiltonian are complicated functions of the angle between a specific direction fixed on the n-proton cluster and the external field. In our NMR work we used powdered samples. The orientation of the crystal grains of which the sample is composed may be considered to be distributed uniformly over all directions. In the previous simulations where two- or three-spin systems were dealt with, we obtained the general solutions from the matrix as the function of the specific angle for the n-proton cluster and the external field, and then simulated the NMR spectra by integrating the solutions over all range of the angle. However, it is difficult to obtain general solutions for the system composed of more than three protons, since the matrix is much more complicated.

In the present work, in spite of integrating general solutions we solved numerically as many matrices (for individual relations among the n-proton cluster's coordinates and the direction of the external fields) as we could and made up a simulated spectra by summing the individual solutions. In the procedure, the coordinates of the protons were fixed and the direction vector of the external field, (1, Θ, Φ), was varied in the following manners to achieve a uniform distribution. The values of Θ and Φ were selected stepwise with a constant increment, $\Delta\Theta$, in the Θ range from 0° to 180° and with a variable increment, $\Delta\Phi$, depending on Θ, which was given by $\Delta\Phi = \Delta\Theta/\sin\Theta$, in the range of $0^\circ \le \Phi < 360^\circ$, respectively.[2] By solving the Hamiltonian matrix we obtained energies ε_l and eigenfunctions of states $|l\rangle$, and then calculated transition energies and transition probabilities from them. The resonance probability of magnetic dipole transition between states l and l' was calculated with $|\langle l|\hat{I}_x|l'\rangle|^2$. The observed transition lines are broadened by neighboring groups. The result was corrected by using a Gaussian broadening function in manner after Pake (24). So an individual line due to a magnetic dipole transition between states l and l' can be treated as a Gaussian peak at $\varepsilon_{l'} - \varepsilon_l$ with a peak area of $|\langle l|\hat{I}_x|l'\rangle|^2$ and a second moment of β. The NMR spectra were obtained as the whole sums of resonance lines calculated for all (1, Θ, Φ) selected. To make the comparison among the systems composed of different numbers of protons possible, the spectra were normalized for their area to be equal to the number of protons contained in respective systems.

Figures 1a–1c show the spectra obtained with different increments of Θ for the proton pairs (0.21 nm of proton separation, 1.3 kHz of the second moment β for the Gaussian function), together with that obtained by the integration of general solutions (Fig. 1d). For all $\Delta\Theta$ values used in Fig. 1 the obtained spectra were almost the same as that by general solutions, except for very little differences near the center of the spectrum for $\Delta\Theta = 6.0^\circ$. This result indicates that the present simulation procedure is available for the lineshape analysis of NMR spectra. The increment $\Delta\Theta = 2^\circ$ was used for our spectral simulation because of expectation of more precise results, although much longer calculation time was needed.

Choice of Models and Fitting Procedure

The protonic sites for type I are known to be on the zigzag chain within the MoO_3 layers, as shown in Fig. 2. Although two available sites exist between the nearest neighbor oxygen atoms of the zig-zag chain, protons cannot

[2]Only $\phi = 0^\circ$ was selected for $\Theta = 0^\circ$ and 180°.

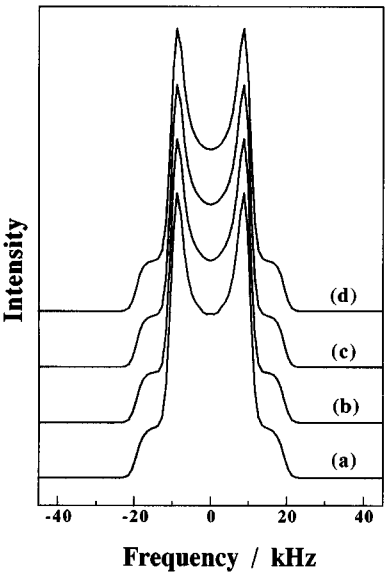

FIG. 1. Simulated spectra for a Pake doublet with protonic separation 0.21 nm. (a)–(c) were obtained by summing individual solutions with $\Delta\Theta$ of 6°, 4°, and 2°, respectively. (d) was by integration of general solutions.

occupy both sites simultaneously. In the previous study we revealed that protons in type I made clusters with neighboring proton separation of ca. 0.21 nm, where the neighboring proton occupies the second nearest site on the zigzag chain (17, 18, 20). In the present study we chose basic clustering models according to these findings. However, we used a different method from the previous one to choose protonic-site arrangements. In the previous study, we varied independently the values for protonic-site separation r_{H-H} and the base angle of the isosceles triangle of the protonic sites for a three-proton system (Fig. 2). Thus, the resultant arrangement gave a slightly larger neighboring proton separation along the c axis ($r_{H-H} \cdot \cos\psi = 0.194$ nm) than the value $c/2$ (0.1868 nm, where c is one of the lattice constants of type I and can be referred to as the unit cell length of the zigzag chain), indicating that protonic sites were not precisely on the zigzag chain, which was along the c axis. For the up to three-proton models dealt with in the previous study, where the size of the cluster was compatible with or less than the length of a unit cell of the chain, the arrangement seemed to be acceptable. However, because of periodicity of the protonic sites, it is not acceptable for the system containing more than three protons, where the cluster might expand on more than one unit cell of the chain. Therefore, in this work we varied only the second-nearest site separation r_{H-H} to arrange the protonic sites and basically treated the angle ψ as a dependent variable of the separation, related by the equation $\cos\psi = 0.1868/r_{H-H}$.[3,4] The proton content of the sample (x = ca. 0.25) corresponds to one-eighth of all the protonic sites in the MoO_3 layer and to one-fourth of the available sites which can be occupied simultaneously. Since protonic density in the type I sample is not so high and so large clusters are not expected, we dealt with up to six-spin systems, the formation of which was suggested in the literature (21).

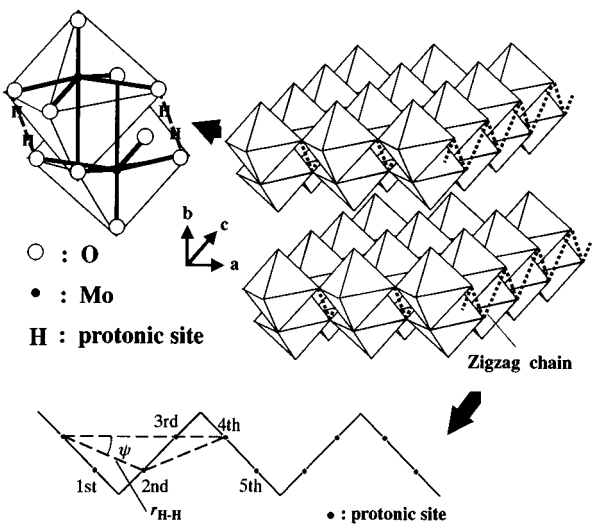

FIG. 2. Schematic model of H_xMoO_3 and sites on the zigzag chain.

Furthermore, in the present work we also dealt with the models arranged in a different manner from that mentioned above. As mentioned in the introduction, Adams *et al.* suggested the formation of six-proton clusters in the phase with $x = 0.33$. Simultaneously they also reported modulation in the Mo–O framework, which leads to a modulated zigzag chain with a variety of O–O distances. The NMR spectra of such clusters on the modulated zigzag chain were simulated. For these clusters, positions of oxygen atoms of the modulated chain were determined according to atomic parameters given by Adams *et al.* (21). Then protonic positions were taken to be on the zigzag chain and determined from the O–H distance. In their paper 0.105 nm O–H distance was suggested. The protonic positions obtained from the distance gave rather shorter H–H distances (0.190–0.201 nm, with a mean value of 0.194 nm), which did not seem to be suitable for reproduction of the observed NMR lineshapes. (The expectable H–H distance is ca. 0.210 mm, as mentioned above.) So we chose the protonic positions varying the O–H distance down to 0.09 nm, which was the shortest distance observed for water in a variety of crystalline hydrates (25). For 0.09 nm O–H distance, H–H distances were in the range 0.197–0.209 nm and their mean value became 0.201 nm.

[3]Other site separations such as the first-nearest or the third-nearest ones were determined from the second-nearest site separation by the symmetrical relations among the sites.

[4]In this work we also dealt with some cases where some protons were not on the zigzag chain (curve e in Fig. 7).

We calculated simulation spectra for many models which consist of several numbers of protons ($n = 1$ to 6), including the six-proton clusters on the modulated zigzag chain, and have various protonic arrangements, varying the value of the second moment β. Then we tried to reproduce the observed spectra by a linear combination of some simulated spectra using a linear least-squares method.

RESULTS AND DISCUSSION

Figure 3 shows the NMR spectra of type I obtained in the present study (Fig. 3a), together with that from the previous study (Fig. 3b) (20). The figures were drawn with the resonance frequency of a free proton taken to be zero kHz. The previous type I sample shows a broad background component due to adsorbed water. However, because we could prepare a type I sample with no adsorbed water, the present sample does not show that component. The present sample also shows the deep dips at both sides of the central peak which cannot be reproduced by systems composed of less than three protons, as in the previous study.

Figures 4b and 4c are the simulation spectra of possible six-proton models with 0.09 nm O–H distance for the modulated zigzag chains given by Adams *et al.* (21), and Fig. 4a is the observed spectrum. Figure 4d gives a spectral combination of the clusters (1), (2), (3), and (4) with molar ratio 0.2 : 0.3 : 0.2 : 0.3 for the respective clusters, and corresponds to a spectrum for an expectable model which can reproduce the protonic site occupancies given by Adams *et al.* (21). The clusters on the modulated zigzag chain apparently give a rather wider peak separation than that in the observed spectrum (Fig. 4a) because of the rather shorter H–H distances of the clusters (0.197–0.209 nm with mean value 0.201 mm) and have not been suggested to be suitable for reproduction of the observed line shapes.

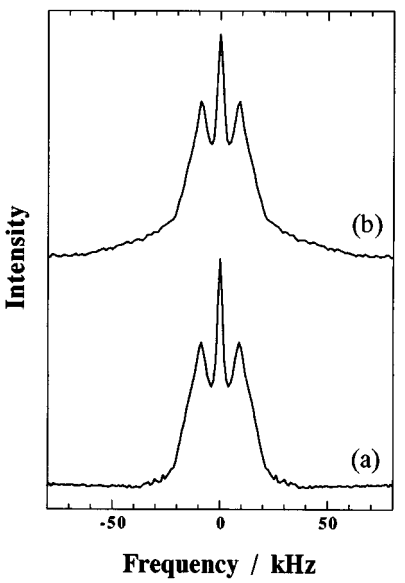

FIG. 3. NMR spectra of type I: (a) this work ($x = 0.26$) and (b) the previous work ($x = 0.25$).

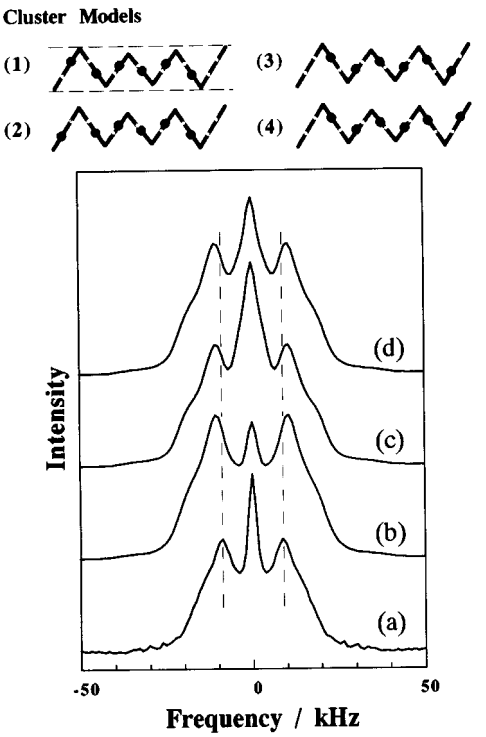

FIG. 4. The six-proton cluster models on the modulated zigzag chains and their simulation spectra: (a) the observed, (b) for models (1) and (3), (c) for models (2) and (4), and (d) for a combination of (b) and (c) with the ratio 0.4 : 0.6.

For the line shape analysis the further absorption spectra of various types of clustering models for normal zigzag chains were simulated. At first the n-proton models ($n = 2$ to 6), where all the protons have a common value of the nearest-neighbor separation, were calculated. Figure 5 shows the models and their simulated spectra (for separation r_{H-H} of 0.207 nm). All the spectra show twin peaks with almost the same peak separation at ca. $\pm$ 10 kHz. The spectra of the systems containing more than two protons showed a central peak with dips at the both sides. There is a tendency for the system with larger number of protons to show broader tails at the edges of absorption and for the lineshape of the spectrum to depend strongly on the number of protons in a system. So we could safely analyze the observed NMR spectra by such models. Figure 6 shows the changes in spectra with the protonic separation for the three-proton system. Because the change in protonic separation (or protonic-site separation) results in the changes in the base angle of the isoceles triangle (the angle is dealt with as a dependent variable of the separation), the spectra

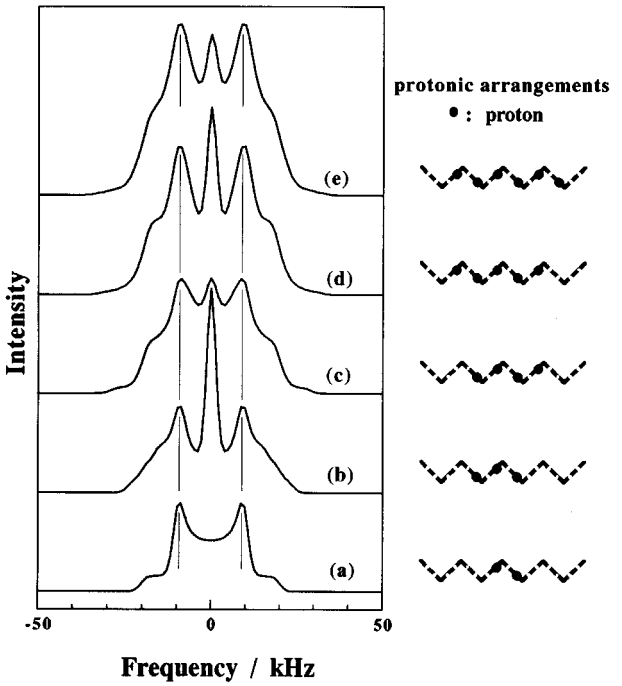

FIG. 5. The n-proton clustering models with a common protonic separation and their simulated spectra. (a)–(e) are for $n = 2, 3, 4, 5$, and 6, respectively. Second-nearest site separation 0.207 nm and 1.3 kHz β were used.

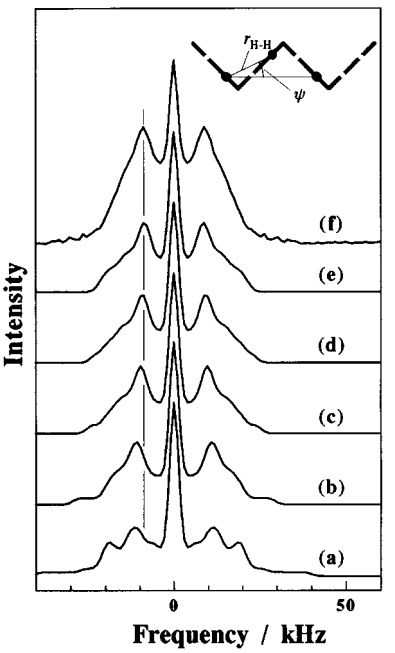

FIG. 6. Spectral changes with protonic separation for three-proton models, where all protons occupy the second-nearest sites. Curves a–e are for $r_{H-H} = 0.190$ ($\psi = 10.5°$), 0.200 (20.9°), 0.205 (24.3°), 0.207 (25.5°), and 0.210 nm (27.2°), respectively. Curve f shows the observed spectrum.

change not only in the peak separation but also in the lineshape. The best reproduction for the twin-peak separation of the observed spectrum was obtained by a model with protonic separation of 0.207 nm. Because the twin-peak separation of the calculated spectra did not depend on the number of protons in the system as shown above (Fig. 5), the value of 0.207 nm was also suitable for the systems with other numbers of protons.

To test further cases, we also calculated the systems in which all protons did not exhibit a common neighboring separation (i.e., some protons occupied other sites than the second-nearest ones). Figure 7 shows the results for the five-proton systems. Curves b and c are obtained for models which consist of two subunits, one composed of three protons and the other of two protons, separated by different distances (all the protons in the subunits have 0.207 nm neighboring separation). The curve a is the spectrum for the model where all the protons have a common value of the neighboring separation (0.207 nm), i.e, the separation between the two subunits is equal to 0.207 nm. Curve d is a simple combination of the separately simulated spectra for two systems with a common neighboring separation of 0.207 nm, composed of three protons and of two protons, respectively. The spectra of the models with 0.374 nm and larger values of the subunit separation became similar to the simple combination of the two systems (curves c and d). The only models with subunit separation 0.207 (the second nearest-site separation) or 0.256 nm (the third-nearest site separation) exhibit apparently different spectra from the simple combination (curves a and b). Corresponding results were also obtained for the models with other numbers of protons and/or with a combination of other types of subunits. The curve e was obtained from the model where both terminal protons are not on the zigzag chain (corresponding to the terminal protons in the three-proton system of the previous study (20), while the three internal protons are on. This curve did not show such large differences from that for the model where all protons are on the chain (curves a and e). The differences were too small for such minor arrangements to be discussed safely and we did not have any information available to choose such arrangements. Moreover, the various models chosen above seemed to be sufficient to discuss whether the 4 to 6-proton cluster existed in type I. So we did not try to make further models where protons in the cluster had different neighboring separations, although such an arrangement might be allowed in real systems.

We tested various combinations of simulated spectra for the various models mentioned above, varying the second moment β of respective components as an adjustable parameter, to reproduce the observed specta. The best fitting for the present type I sample was obtained by the combination of systems of three, four, and five protons, with a consequent

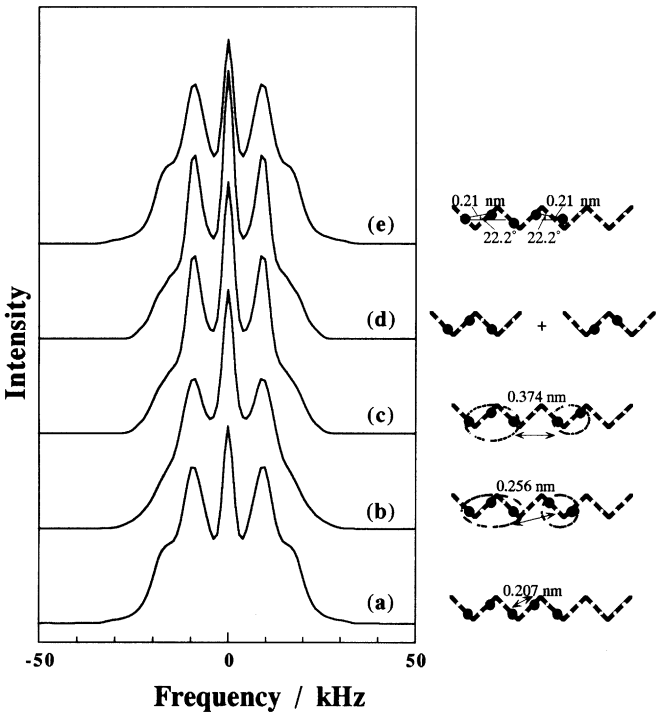

FIG. 7. Several five-proton models with various protonic arrangements and their simulated spectra. Second-nearest site separation 0.207 nm and 1.3 kHz β were used.

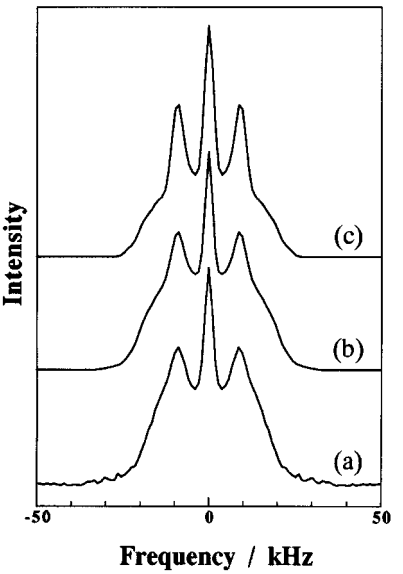

FIG. 8. (a) The experimental and (b), (c) simulated lineshapes of proton NMR spectrum for type I. (b) was obtained by lineshape analysis using all linesshapes calculated for up to 6-proton systems ($n = 1$ to 6), and (*c*) was obtained using lineshapes for up to three-proton systems ($n = 1$ to 3).

molar ratio of 1 : 1.4 : 0.3 for three-, four-, and five-proton clusters, where all protons in the systems had the same neighboring proton separation (0.207 nm).[5] The results are shown in Fig. 8, together with the result for the combination of two- and three-proton systems referred in the previous study.[6] From an inspection it is clear that the former fitting is much better than the latter. This result suggests that four- or five-proton clusters are formed in type I.[7]

CONCLUSION

We developed a new program for simulation of powder NMR spectra which could deal with systems containing more than three protons. The program gives the simulated spectra by summing the solutions for uniformly distributed discrete directions, in spite of integrating the solutions over all directions. The procedure seemed slightly rough, but we found that it could give almost the same spectra as integration. So we simulated various models containing systems with more than three protons using the program and tried to reexamine the protonic locations in type I by comparison with observed lineshapes. We found that 4- and 5-proton clusters also played an important role in type I. The spectra for the 6-proton clusters on the modulated zigzag chains, which were suggested to be formed in phase I by Adams *et al.*, were also calculated, but were not suitable to reproduce the observed line shapes.

[5]The six-proton models on the normal zigzag chains gave a slightly wider skirt around $\pm$ 20 kHz than that in the observed spectrum and were not suitable for the expectable models for the phase I.

[6]The used second moments for the three-, four-, and five-proton models in Fig. 8b are 1.0, 2.0, and 2.0 kHz, respectively. The consequent molar ratio is 1 : 1.3 for two- (the second moment $\beta = 1.3$ kHz) and three-proton ($\beta = 1.3$ kHz) models in Fig. 8c.

[7]The NMR spectrum in the previous study was also reanalyzed and the result supported this suggestion.

REFERENCES

1. O. Glemser and G. Lutz, *Z. Anorg. Allgem. Chem.*, **264,** 17 (1951).
2. O. Glemser, U. Hauschild, and G. Lutz, *Z. Anorg. Allgem. Chem.* **269,** 93 (1952).
3. O. Glemser, G. Lutz, and G. Meyer, *Z. Anorg. Allgem. Chem.* **285,** 173 (1956).
4. J. J. Birtill and Dickens, *Mater. Res. Bull.* **13,** 311 (1978).
5. N. Sotani, K. Eda. M. Sadamatsu, and S. Takagi, *Bull. Chem. Soc. Jpn.* **62,** 903 (1989).
6. P. G. Dickens, J. J. Birtill, and C. J. Wright, *J. Solid State Chem.* **28,** 185 (1979).
7. P. G. Dickens, S. J. Hibble, and G. S. Games, *Solid State Ionics* **20,** 213 (1986).
8. P. G. Dickens, A. T. Short, and S. Crouch-Baker, *Solid State Ionics* **28–30,** 1294 (1988).
9. R. C. T. Slade, P. R. Hirst, B. C. West, R. C. Ward, and A. Magerl, *Chem. Phys. Lett.* **155,** 305 (1989).

10. R. C. T. Slade, P. R. Hist, and H. A. Pressman, *J. Mater. Chem.* **1,** 429 (1991).
11. J. B. Parise, E. M. McCarron III, and A. W. Sleight, *Mater. Res. Bull.*, **22,** 803 (1987).
12. F. A. Schröder and H. Weitzel, *Z. Anorg. Allgem. Chem.*, **435,** 247 (1977).
13. A. Cirillo and J. J. Fripiat, *J. Phys.* (*Paris*) **39,** 247 (1978).
14. A. Cirillo, Jr., L. Ryan, B. C. Gerstein, and J. J. Fripiat, *J. Chem. Phys.* **73,** 3060 (1980).
15. R. E. Taylor, M. M. Silva Crawford, and B. C. Gerstein, *J. Catal.* **62,** 401 (1980).
16. R. C. T. Slade, T. K. Halstead, and P. G. Dickens, *J. Solid State Chem.* **34,** 183 (1980).
17. Cl. Ritter, W. Müller-Warmuth, H. W. Spiess, and R. Schöllhorn, *Ber. Bunsenges. Phys. Chem.* **86,** 1101 (1982).
18. Cl. Ritter, W. Müller-Warmuth, and R. Schöllhorm, *J. Chem. Phys.* **83,** 6130 (1985).
19. N. Sotani, K. Eda, and M. Kunitomo, *J. Chem. Soc. Faraday Trans.* **86,** 1583 (1990).
20. M. Kunitomo, K. Eda, N. Sotani, and M. Kaburagi, *J. Solid State Chem.* **99,** 350 (1992).
21. S. Adams, K-H. Ehses, and J. Spilker, *Acta Crystallogr. Set. B* **49,** 958 (1993).
22. R. Rousseau, E. Canadell, P. Alemany, D. Galvan, and R. Hoffmann, *Inorg. Chem.* **36,** 4627 (1997).
23. A. Abragam, "The Principles of Nuclear Magnetism", Oxford, London, 1961.
24. G. E. Pake, *J. Chem. Phys.* **16,** 327 (1948).
25. M. Falk and O. Knop, *in* "Water" (Felix Franks Ed.), Vol. 2, Ch. 2, pp. 64–69. Plenum Press, New York, 1973.